Journal of Applied Polymer Science

Complex of Cisplatin with Biocompatible Poly(ethylene glycol) with Pendant Carboxyl Groups for the Effective Treatment of Liver Cancer

Jing Li,[1] Xiuli Hu,[1] Ming Liu,[1] Jie Hou,[2] Zhigang Xie,[1] Yubin Huang,[1] Xiabin Jing[1]

[1]State Key Laboratory of Polymer Physics and Chemistry, Changchun Institute of Applied Chemistry, Chinese Academy of Sciences, Changchun 130022, People's Republic of China

[2]The First Hospital of Jiamusi University, Jiamusi, 154002, People's Republic of China

Correspondence to: Z. Xie (E-mail: xiez@ciac.ac.cn)

ABSTRACT: Cisplatin was incorporated into polymeric carriers through the coordination of Pt with the carboxylic groups of methoxy-poly(ethylene glycol) (mPEG)-*block*-poly[(2-carboxy-ethylsulfanyl)-propyl glycidyl ether] (PCPGE). The mPEG-*b*-PCPGE/Pt complexes with a Pt content of 14 wt % could self-assemble into spheric micelles with diameter of about 80 nm in aqueous solution. The effective internalization of the polymer platinum micelles by the cells via an endocytosis mechanism was confirmed by confocal laser scanning microscopy and flow cytometry. The antitumor activity of the polymeric micelles was similar to that of cisplatin *in vitro*. The *in vivo* blood clearance of platinum was studied, and the results show that the micelles exhibited longer blood circulation than the free cisplatin. The biodistribution of cisplatin and its micelles in mice was studied through the measurement of the Pt content in plasma, organs, and tumors, especially in tumor cell DNA. Their antitumor activity *in vivo*, assessed in mice bearing H22 liver cancers, showed that the micelles exhibited greater antitumor efficacy than free cisplatin. Therefore, this polymer platinum micelle is a promising candidate as a smart antitumor drug carrier for malignancy therapy in future clinical applications. © 2014 Wiley Periodicals, Inc. J. Appl. Polym. Sci. **2014**, *131*, 40764.

KEYWORDS: biomedical applications; drug-delivery systems; micelles

Received 30 October 2013; accepted 24 March 2014
DOI: 10.1002/app.40764

INTRODUCTION

Cisplatin, carboplatin, oxaliplatin, and other platinum(II)-based drugs are widely used in cancer chemotherapy and have greatly improved the prognosis for ovarian, lung, and especially testicular cancers.[1–4] To improve the therapeutic index of platinum drugs, two strategies have emerged. The first approach is the design and development of new platinum complexes that modulate the molecular process and pathways specifically associated with tumor progression. Alternatively, existing platinum drugs can be modified effectively with nanocarriers. Nanocarriers could bring more drug molecules to tumor sites and reduce the exposure of normal tissues to the drugs. Recently, enormous efforts have been dedicated to the development of polymeric Pt complexes.[5–11] These efforts are expected to overcome the side effects by prolonging the systematic circulation and to target drugs to tumor sites via passive and active targeting.[12–22]

For polymeric Pt(II) complexes, the most investigated drugs are cisplatin and oxaliplatin. The used polymer carriers include chitosan,[23] dendrimers,[24] *N*-(2-hydroxypropyl) methacrylamide copolymers,[25] polyaspartamide,[26] and polyglutamide polymers.[27] However, most of these carrier polymers have a high polydispersity and are hard to synthesize. Poly(ethylene glycol) (PEG) is usually synthesized by anion ring-opening polymerization, and it has a low polydispersity index (<1.10). PEG is widely used in the pharmaceutical and biomedical fields today. However, the low loading capacities at the chain end limit the application of PEG. The synthesis of PEG with multiple functional groups along the backbone was developed via different methods. Frey and coworkers[28,29] reported the synthesis of poly(ethylene glycol-*co*-ally glycidyl ether)s and their further modification via thiol-ene coupling. In their study, the methoxy-poly(ethylene glycol) (mPEG)-*block*-poly[(2-carboxy-ethylsulfanyl)-propyl glycidyl ether] (PCPGE) with pendant carboxyl groups was used as the drug carrier.

A promising carrier for platinum drugs is polymeric micelles.[30–33] Polymeric micelles, which are self-assembled block copolymers with a core–shell structure, have several useful functions that benefit the protection and targeted delivery of platinum drugs.[34,35] They usually enter the cancer cells via endocytosis with considerable efficiency. The carrier polymer can be degraded, and the encapsulated drugs can be rapidly released under the endosome or secondary lysosome conditions. The first

platinum-drug-loaded micelle was reported by Kataoka et al.[35] and was prepared by the metal-complex formation between cisdichlorodiamine platinum(II) (cisplatin) or dichloro (1,2-diaminocyclohexane) platinum (II) (DACH)-Pt and PEG-*b*-poly(amino acid) block copolymers.

Our previous studies indicated that polymeric micelles showed remarkably prolonged blood circulation and greater accumulation in tumor tissue compared to a free platinum drug,[36,37] but all of these polymeric carriers are amphiphilic block copolymers and are synthesized via cumbersome multistep reactions. For example, the copolymer PEG-*block*-poly(L-lactide-*co*−2-methyl-2-carboxyl-propylene carbonate) is synthesized by the copolymerization of lactide and 2-methyl-2-benzoxycarboxyl-propylene carbonate and subsequent catalytic hydrogenation.[32,37] Moreover, these drug carriers usually have a high polydispersity; this is a disadvantage for clinical drug approval because of its structural uncertainty. It is highly desirable to develop simple polymer carriers with a low dispersity for drug encapsulation or conjugation.

In this study, polymeric micelles were prepared by the complexing of mPEG-*b*-PCPGE with cisplatin. The copolymer mPEG-*b*-PCPGE was easily prepared with a low polydispersity. This water-soluble mPEG-*b*-PCPGE became amphiphilic and could form micelles after coordination with platinum; this was the biggest difference between this study and previous work.[37] The platinum was not just an anticancer drug; it also crosslinked the polymeric micelles to increase the stability of the nanoparticles. The micellar physicochemical characteristics, such as their particle size, size distribution, and drug loading, were characterized. The *in vitro* drug release and uptake by the cells was studied in detail. The *in vivo* behaviors, such as the blood clearance, biodistribution, and antitumor activity, were measured with Kunming mice bearing H22 liver cancer.

EXPERIMENTAL

Materials

PEG monomethyl ether (number-average molecular weight = 2000 g/mol), ally glycidyl ether, 3-mercapto-propanoic acid (MPA), and cesium hydroxide monohydrate (99.9%) were all purchased from Sigma-Aldrich (China). Cisplatin (purity = 99.0%) was purchased from Shandong Boyuan Pharmaceutical Co., Ltd. (China). The block copolymer mPEG-*b*-PAGE was synthesized according to the literature. All of the other chemicals and solvents were obtained commercially and were used without further purification.

Measurements

^{1}H-NMR spectra were measured by a Unity 300-MHz NMR spectrometer (Bruker, Germany) at room temperature. Mass spectroscopy (MS)–electrospray interface measurements were performed on a Quattro Premier XE system (Waters) equipped with an electrospray interface. Matrix-assisted laser-desorption ionization time-of-flight (MALDI-TOF) MS (Waters) was used to study the chelation of the Pt species with 5′-guanosine monophosphae (GMP). An inductively coupled plasma optical emission spectrometer (iCAP 6300, Thermoscientific) was used to determine the total platinum contents in the polymer–Pt(IV) conjugate, and samples were obtained outside of the dialysis bags in the drug-release experiments. Inductively coupled plasma mass spectroscopy (ICP-MS; Xseries II, Thermoscientific) was used for the quantitative determination of trace levels of platinum. The size and size distribution of the micelles were determined by dynamic light scattering (DLS) with a vertically polarized He–Ne laser (DAWN EOS, Wyatt Technology). The morphology of the polymer–Pt(IV) micelles was measured by transmission electron microscopy (TEM) with a JEOL JEM-1011 electron microscope.

Synthesis of mPEG-*b*-PCPGE

The block copolymer mPEG-*b*-PAGE was synthesized according to the literature.[37] To introduce carboxyl groups, MPA was used to react with the mPEG-*b*-PAGE by thio-ene reaction. The mPEG-*b*-PAGE (0.1 g, 0.032 mmol) and MPA (0.14 mL, 1.6 mmol) were dissolved in 10 mL of tetrahydrofuran in a 100-mL, round-bottomed quartz flask; this was followed by degassing with N_2 for 30 min to eliminate the dissolved oxygen. Then, the mixture was stirred at room temperature under UV light (254 nm, 1.29 mW/cm^2). After 8 h, the light source was turned off, and the mixture was concentrated *in vacuo*. The residues were poured into large amounts of cold diethyl ether to cause precipitation and to give the final product, mPEG-*b*-PCPGE (yield = 90%).

Preparation of the Methoxy-Poly(ethylene glycol)-*b*-Poly[(2-carboxy-ethylsulfanyl)-propyl glycidyl ether]/Pt [M(Pt)] Micelles

The cisplatin (0.5 g, 1.67 mmol) was suspended in distilled water and mixed with silver nitrate ($AgNO_3$/cisplatin = 2 mol/mol) to form an aqueous complex. The solution was kept in the dark at room temperature for 12 h. The AgCl precipitates formed during the reaction were removed by centrifugation. The supernatant $[(NH_3)_2Pt–(H_2O)_2(NO_3)_2]$ was filtered for further purification.

An amount of 0.61 g of mPEG-*b*-PCPGE (1.4 mmol carboxyl groups) was added to 20 mL of double-distilled water and stirred for 30 min at room temperature; this was followed by the addition of 0.22 g of Na_2CO_3 to deprotonate the carboxyl groups. Thereafter, the previous $(NH_3)_2Pt–(H_2O)_2(NO_3)_2$ aqueous solution was added to the polymer solution, and the reaction mixture was stirred vigorously for 24 h in an ice–water bath. Then, the complex solution was dialyzed against deionized water with a dialysis bag with a molecular weight cutoff of 3500 for 12 h.

To determine the drug-loading content (LC w/w %) of the micelles, the cisplatin-loaded micelle solution was lyophilized and then dissolved in deionized water by ultrasonication for 15 min. The Pt content was measured with ICP-MS. The LC values of the micelles were then calculated with the following formula:

$$\text{LC}\,(\%) = \text{Drug loading}\,(\text{g}) \times 100 / \text{Content of dry polymer disk}\,(\text{g}).$$

The drug content in the micelles was 14 wt %.

Synthesis of the Rhodamine B (RhB)-Labeled Copolymer mPEG-*b*-PCPGE/Pt [M(Pt)–RhB]

Amounts of 0.5 g of mPEG-*b*-PCPGE/Pt and 0.001 g of RhB were dissolved in 10 mL of methylene chloride; this was followed by the addition of 0.17 g of *N*,*N*′-dicyclohexylcarbodiimide and

0.05 g of DMAP (4-dimethylaminopyrridine), respectively. The reaction mixture was kept stirring in an ice bath for 24 h, filtered, and precipitated with excess diethyl ether. The RhB-labeled polymer [M(Pt)–RhB] was collected and vacuum-dried.

Observation of the M(Pt) Micelles by TEM and DLS

An M(Pt) micellar solution (0.2 mg/mL, 10 mL) was prepared, and the micelles were observed by TEM (JEOL JEM-1011 electron microscope). The size distribution of the micelles was determined by dynamic light scattering with a vertically polarized He–Ne laser (DAWN EOS, Wyatt Technologies). The scattering angle was fixed at 90°, and the measurement was carried out at a constant temperature of 25°C. The sample solutions were diluted in filtered double-distilled water before analysis.

Drug Release from the M(Pt) Micelles

An amount of 3 mg of lyophilized M(Pt) micelles (M, Pt content = 14%) was dissolved in 5 mL of buffered solution [100 m*M* phosphate-buffered saline (PBS) at pH 7.4 and 10 m*M* acetate-buffered solution at pH 5.0). The solution was then placed into a preswollen dialysis bag with a molecular weight cutoff of 3.5 kDa and immersed in 35 mL of buffered solution. The dialysis was conducted at 37°C in a shaking culture incubator. A volume of 1 mL of the sample solution was withdrawn from the incubation medium at specified time intervals and measured for Pt concentration by ICP-MS. After sampling, an equal volume of fresh buffered solution was immediately added to the incubation medium. The platinum released from the micelles was expressed as the percentage of cumulative platinum outside the dialysis bag relative to the total platinum in the micelles.

Biocompatibility Assay

Human liver hepatocellular carcinoma (HepG2) cells harvested in a logarithmic growth phase were seeded in 96-well plates at a density of 1×10^5 cells/well and incubated in Dulbecco's modified Eagle's medium (DMEM) for 24 h. The medium was then replaced by DMEM solution at final equivalent concentrations from 0.896 to 700 μg/mL. The incubation was continued for 48 h. Then, 20 μL of 3-(4,5-dimethylthiazol-2-yl)-2,5-diphenyltetrazolium bromide (MTT) solution in PBS with a concentration of 5 mg/mL was added, and the plates were incubated for another 4 h at 37°C; this was followed by the removal of the culture medium containing MTT and the addition of 150 μL of dimethyl sulfoxide to each well to dissolve the formazan crystals formed. Finally, the plates were shaken for 10 min, and the absorbance of formazan product was measured at 570 nm by a microplate reader.

Cytotoxicity Assay

HepG2 cells harvested in a logarithmic growth phase were seeded in 96-well plates at a density of 1×10^5 cells/well and incubated in DMEM for 24 h. The medium was then replaced by cisplatin and M(Pt) micelle solutions in DMEM at a final equivalent Pt concentration from 0.064 to 100 μg/mL. The incubation was continued for 48 h. Then, 20 μL of MTT solution in PBS with a concentration of 5 mg/mL was added, and the plates were incubated for another 4 h at 37°C; this was followed by the removal of the culture medium containing MTT and the addition of 150 μL of dimethyl sulfoxide to each well to dissolve the formazan crystals that formed. Finally, the plates were shaken for 10 min, and the absorbance of the formazan product was measured at 570 nm by a microplate reader. Cell viability was calculated with the MTT absorbance of the control and treated cells:

$$\%\ \text{Survival} = (\text{Mean value of the treated sample} / \text{Mean value of the untreated sample}) \times 100.$$

Cellular Uptake of the M(Pt) Micelles

The HepG2 cells were grown in DMEM with 10% fetal bovine serum at 37°C in 5% CO_2. HepG2 cells harvested in a logarithmic growth phase were seeded in six-well plates at a density of 1×10^6 cells/well and incubated in DMEM for 24 h. The medium was then replaced by cisplatin and M(Pt) micelle solutions at a final equivalent Pt concentration of 5 mg/mL for each drug. The HepG2 cells were harvested 30 min and 2 h posttreatment, and genomic DNA was isolated with a Takara DNA extraction kit (Takara Mirus Bio, Dalian, China). The final DNA pellet was air-dried and then dissolved in 0.3 mL of distilled water overnight. The DNA concentration and purity were determined by the measurement of the absorbance at 260/280 nm with a NanoDrop UV spectrometer (NanoDrop Technologies, Inc., Wilmington, DE). The Pt concentration was then determined by ICP-MS.[38] The total Pt–DNA adducts were expressed as nanograms of Pt per micrograms of DNA.

Confocal Laser Scanning Microscopy (CLSM)

Cellular uptake by the HepG2 cells was examined with CLSM. The HepG2 cells were seeded in six-well culture plates (a sterile cover slip was put into each well) at a density of 2×10^4 cells per well and allowed to adhere for 24 h. After that, the cells were treated with M(Pt) micelles with RhB (0.5 mg/mL) for 0–180 min at 37°C. After that, the supernatant was carefully removed, and the cells were washed three times with PBS. Subsequently, the cells were fixed with 800 μL of 4% formaldehyde in each well for 20 min at room temperature and washed twice with PBS again. The slides were mounted and observed with a confocal scanning microscope imaging system. 4′,6-Diamidino-2-phenylindole was used to stain the nuclei.

Flow Cytometry Scanning (FCS)

Cellular uptake by HepG2 cells was examined with FCS. The HepG2 cells were seeded in six-well culture plates at a density of 5×10^4 cells per well and allowed to adhere for 24 h. After that, the cells were treated with M(Pt) micelles with RhB (0.5 mg/mL) for 0–180 min at 37°C. Thereafter, the culture medium was removed, and the cells were washed with PBS three times and treated with trypsin. Then, 1.0 mL of PBS was added to each culture well, and the solutions were centrifuged for 5 min at 5000 rpm. After the removal of the supernatants, the cells were resuspended in 0.5 mL of PBS. Data for the 10,000 gated events were collected, and analyses were performed by flow cytometry (Beckman, California).

Blood Clearance

To develop the tumor xenografts, mouse hepatoma H22 cells (5×10^6 cells in 0.1 mL of PBS) were injected into the lateral

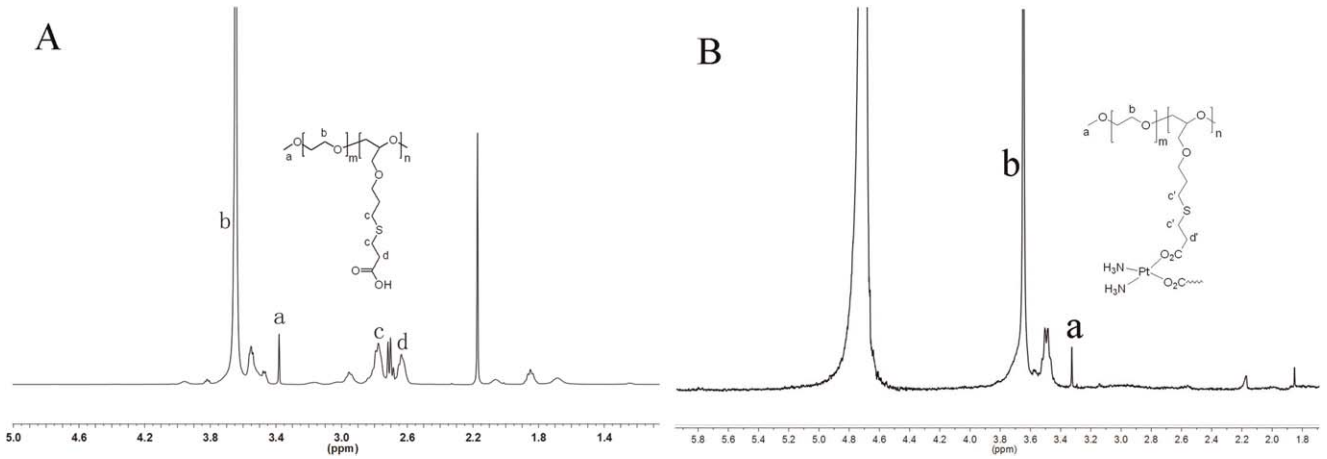

Figure 1. ^{1}H-NMRof the (A) MPEG2k–PCPGE in $CDCl_3$ and (B) M(Pt) micelles in D_2O.

aspect of the anterior limb of the mice. After the tumor volume reached 50–200 mm^3, the hair of the mice was removed with a sodium sulfide solution (80 g/L in 30 vol % aqueous alcohols). Twenty-two kunming (KM) mice were randomly divided into two groups. The mice were injected with cisplatin or M(Pt) micelles via a tail vein, respectively, with an equivalent Pt dose of 5 mg/kg of body weight. Blood samples were collected in heparinized tubes right after injection (with the time point set as 5 s) and at different time intervals after administration (5 min, 10 min, 15 min, 30 min, 1 h, 3 h, 6 h, 9 h, 12 h, and 24 h). Subsequently, the blood samples were completely dissolved into 65% v/v nitric acid with heating, and the platinum contents were measured by ICP-MS. To directly show the clearance of the micelles from blood, the micelle quantity, expressed as a percentage of the injected dose (% ID), was plotted as a function of time.

Biodistribution

Twelve KM mice were randomly divided into cisplatin and M(Pt) micelle groups. The mice were injected with cisplatin and M(Pt) micelle solutions via a tail vein, respectively (with an equivalent Pt dose of 5 mg/kg of body weight) and then sacrificed at 1, 3, 6, and 24 h. Major organs and tissues, including the heart, liver, spleen, kidneys, and tumors, were collected and washed with 0.9% saline before weighing. The organs were dissolved in 65% v/v nitric acid at 60°C for 2 h, and the Pt concentrations were measured by ICP-MS.

Antitumor Efficacy

Fifteen mice bearing H22 tumor nodules were randomly divided into three groups: (1) normal saline (blank control), (2) cisplatin, and (3) M(Pt) micelle. Before injection, all of the mice were marked and weighed, and the length and width of the tumor were measured as the initial size on day 1. The day of the starting injection was designated as day 1. For groups 2 and 3, an equivalent Pt dose of 3 mg/kg of body weight was intravenously injected via a tail vein on days 1, 3, and 5, separately. For group 1, the mice were injected with an equivalent volume of normal saline. The tumor size was measured every other day, and its volume was calculated ($a \times b^2 \times 0.5$, where a is the largest diameter and b the smallest diameter). The mouse survival rate in each group was recorded daily.

Statistical Analysis

The data were expressed as the mean plus or minus the standard deviation. A Student's t test was used to determine the statistical difference between various experimental and control groups. The differences were considered statistically significant at a level of $p < 0.05$.

RESULTS AND DISCUSSION

Preparation of mPEG-*b*-PCPGE

Recently, various functional PEGs were reported for the preparation of drug-delivery systems. For example, poly(ethylene glycol-*co*-allylglycidyl ether)s were synthesized by the anionic ring-opening polymerization of ethylene oxide and allylglycidyl ether.[28,29] Here, we used the functional PEG to make block polymer micelles for drug delivery. First, the copolymer mPEG-*b*-PAGE was made by controlled anionic ring-opening polymerization with a low polydispersity.[39] The molecular weights of the PEG and PAGE blocks determined by ^{1}H-NMR were 2000 and 1140 g/mol, respectively. Then, the allyl groups on the PAGE block were converted to carboxyl groups via a thio-ene reaction with MPA, and the carboxyl groups were used to coordinate with platinum.[39] The ^{1}H-NMR spectrum of mPEG-*b*-PCPGE in $CDCl_3$ is shown in Figure 1. The characteristic peaks of mPEG-*b*-PCPGE at 2.62 and 2.78 ppm assigned to the methylene protons adjacent to carboxylic groups provided evidence for the successful polymerization of the ally glycidyl ether monomer and the conversion of the allyl groups into carboxyl groups.

Preparation and Characterization of the M(Pt) Micelles

The M(Pt) micelles were prepared by the complexation of $(NH_3)_2Pt$–$(H_2O)_2(NO_3)_2$ with the carboxyl on the mPEG-*b*-PCPGE chains. First, $(NH_3)_2Pt$–$(H_2O)_2(NO_3)_2$ was made by the reaction of cisplatin with aqueous $AgNO_3$. What should be pointed out is that the mPEG-*b*-PCPGE was soluble in water, but the block of PCPGE became water-insoluble after complexation with platinum. As shown in Scheme 1, a polymeric micelle with a core–shell structure was formed in an aqueous

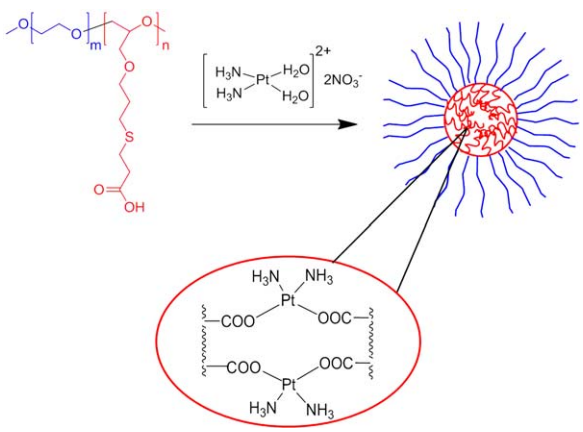

Scheme 1. Preparation of the M(Pt) micelles. [Color figure can be viewed in the online issue, which is available at wileyonlinelibrary.com.]

solution. Moreover, the cisplatin could coordinate with the carboxyl groups on different polymer chains, and this led to the crosslinking of the micelles. This increased the stability of the M(Pt) micelles in blood circulation.

The size and morphology of the M(Pt) micelles in aqueous solution were examined by TEM and DLS. As shown in Figures 2 and 3, nanoscale spherical particles were formed with a diameter of 80 nm as determined by TEM; this was a little smaller than that determined by DLS because of micelle shrinkage during the TEM sample preparation.

Drug Release from the M(Pt) Micelles

Drug-release experiments from the M(Pt) micelles were performed at different pH values. ICP-MS was used to determine the amount of platinum released. The weight percentage of cumulative released platinum with respect to the total platinum payload in the micelles was measured as a function of the release time. As shown in Figure 4, the platinum release at pH 5.0 showed little difference with that at pH 7.4. M(Pt) micelles are actually a polymeric prodrug. Only when the platinum species is released from the micelles can it perform its antitumor activity. The possible reason for this similar drug-release behaviors was the coordination bond between the platinum and polymer carriers was not dependent on the pH value of the aqueous solution. Although the release was only run for 48 h, this result actually proved that the crosslinking by platinum was not unbreakable. As we know, an ideal drug-delivery system should be stable enough to block drug release in the blood circulation and release its payload at the target. The release experiments showed that the platinum species could be released in PBS.

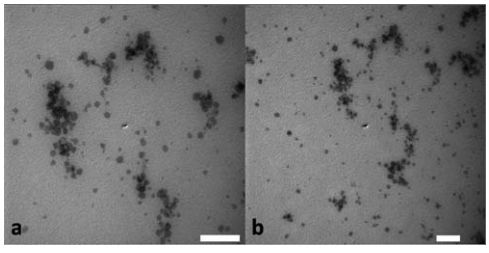

Figure 2. TEM images of the M(Pt) micelles (scale bars = 200 nm).

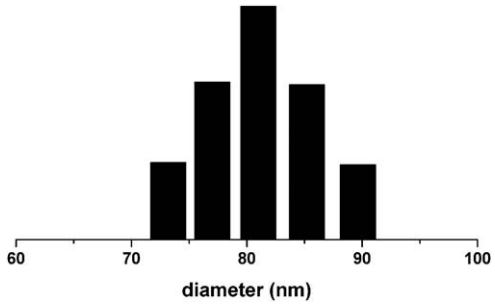

Figure 3. M(Pt) micelles sizes as determined by DLS.

In Vitro Cytotoxicity of the M(Pt) Micelles

The biocompatibility or toxicity of mPEG-*b*-PCPGE was important and needed to be checked before the evaluation of the cytotoxicity of the M(Pt) micelles. The *cytotoxicity* is the degree to which an agent has specific destructive action against certain cells, whereas *biocompatibility* is the property in which the agent is biologically compatible and does not produce a toxic, injurious, or immunological response in living tissue. Biocompatibility is preferably referred to a material, whereas cytotoxicity is related to a drug. To evaluate the effect of mPEG-*b*-PCPGE on the growth and apoptosis of HepG2 cells and to determine the material biocompatibility. As shown in Figure 5, the viability of the HepG2 cells was more than 90% at all test concentrations up to 0.7 mg/mL; this indicated a low toxicity and good compatibility of the mPEG-*b*-PCPGE with the HepG2 cells.

To examine the cytotoxicity of the cisplatin and M(Pt) micelles, the HepG2 cells were exposed to them in six Pt doses (0.064–100 μg/mL) for 48 h, and an MTT assay was performed afterward. As for the cytotoxicity of the two drug formulations, the following variation tendencies were outlined from Figure 6. (1) cisplatin and M(Pt) all showed a dose-dependent cytotoxicity toward the two cancer cell lines examined: a higher dose of Pt drugs induced greater cell inhibition, and (2) the M(Pt) micelles [concentration causing 50% inhibition (IC_{50}) = 8.1 μg/mL] were almost as same as cisplatin (IC_{50} = 7.9 μg/mL) for the HepG2 cells. These data indicated that the micelles exhibited similar cytotoxicity as cisplatin against the HepG2 cells.

Cellular Uptake

Of the two drugs, the M(Pt) micelles were more effective as far as drug-internalization was concerned because of their well-known intracellular uptake mechanism via the endocytosis of

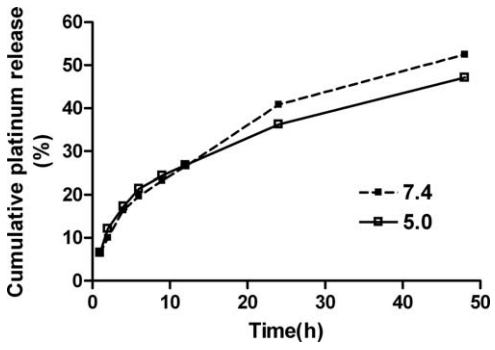

Figure 4. Drug-release profiles of the M(Pt) micelles at pH 5.0 and 7.4.

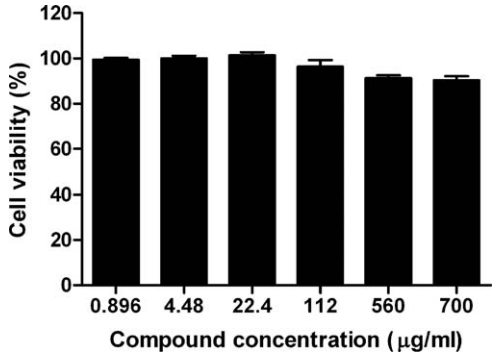

Figure 5. *In vitro* biocompatibility of mPEG-*b*-PCPGE against HepG2 cells at 48 h.

the macromolecular drugs rather in contrast to the free diffusion of free cisplatin. To visualize the M(Pt) micelles taken up by the HepG2 cells, the HepG2 cells incubated with RhB-labeled M(Pt) micelles (0.5 mg/mL) were examined by CLSM and FCS. The fluorescent RhB served as a probe for the polymeric micelles. Figures 7 and 8 show the CLSM images and flow cytometric profiles of the HepG2 cells at 0, 10, 30, 60, 120, and 180 min postadministration of the drugs. Because the cells were thoroughly washed, the fluorescence of RhB was believed to come from the micelles placed inside the cells. As shown in Figures 7 and 8, from 0 to 180 min, the red fluorescence intensity inside the cells increased in a time-dependent manner; this suggested that more and more micelles were internalized, and the rate of endocytosis of the M(Pt) micelles was quite high. The CLSM images further showed that the red fluorescence was full of cell plasma. This indicated that the micelles entered the cells efficiently (Figure 7).

We also quantified the levels of the Pt present in cell DNA from the internalized M(Pt) micelles and free cisplatin. The HepG2 cells were incubated with free cisplatin and M(Pt) micelles for 0.5 and 2 h. This was followed by the collection and purification of the total DNA of the treated cells and the measurement of the Pt concentration in DNA with ICP-MS. As shown in Figure 9, the Pt contents of the M(Pt) micelles and cisplatin in the cells were 51,013 and 15,752 ng of Pt/μg of DNA, respectively, for the HepG2 cells incubated for 2 h. The Pt content in the DNA from the HepG2 cells were in the order Cisplatin < M(Pt) micelles for 2 h. It is well-known that platinum drugs can cause apoptosis of

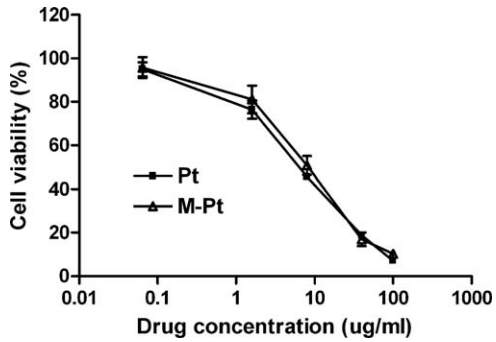

Figure 6. Cell viabilities of the HepG2 cells after 48 h of incubation with the cisplatin (Pt) and M(Pt) micelles at various equivalent Pt concentrations.

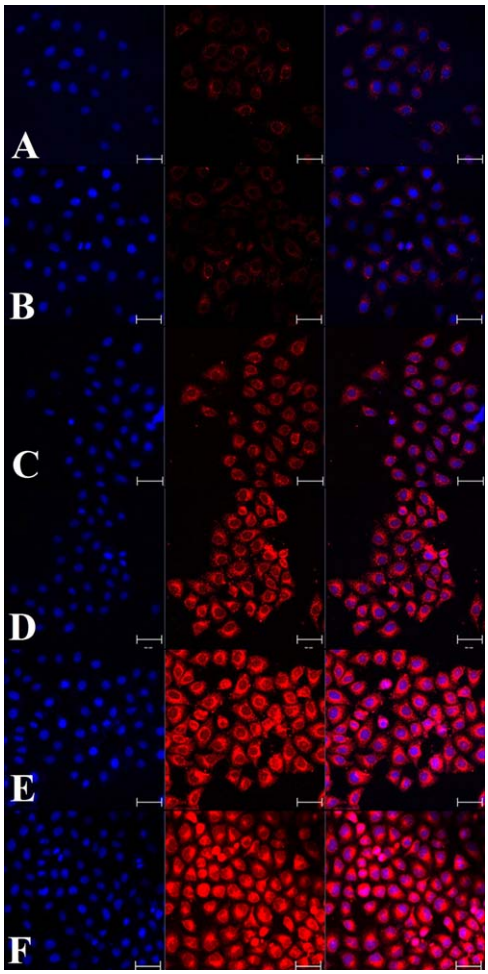

Figure 7. CLSM images of the HepG2 cells after (A) 0, (B) 10, (C) 30, (D) 60, (E) 120, and (F) 180 min of incubation with the M(Pt) micelles labeled with RhB (scale bar = 50 μm). For each panel, the microimages from top to bottom show cellular nuclei stained by 4′, 6-diamidino-2-phenylindole (blue), RhB fluorescence in cells (red), and the overlays of the two microimages. [Color figure can be viewed in the online issue, which is available at wileyonlinelibrary.com.]

cancer cells via chelation with the DNA strands to form Pt–DNA adducts. Therefore, the Pt content in the DNA sample was a measure of the amount of platinum that was really responsible for cell death or, in short, the therapeutically effective amount of platinum. Therefore, the data in Figure 9 convincingly supported the effectiveness order M(Pt) micelles > Cisplatin.

Plasma Pharmacokinetics

The Pt concentration in plasma was determined as a function of time after a single injection of cisplatin and M(Pt) micelles (with an equivalent Pt content of 5 mg of Pt/kg of body weight) into mice bearing H22 liver cancers. As shown in Figure 10, the plasma platinum content after the injection of cisplatin and the M(Pt) micelles decayed in a biexponential manner, and the plasma clearance of the M(Pt) micelles was much slower than that of free cisplatin. Notably, the M(Pt) micelles revealed a significantly longer circulation time than free cisplatin; during this time, the concentration of Pt in the plasma decreased to

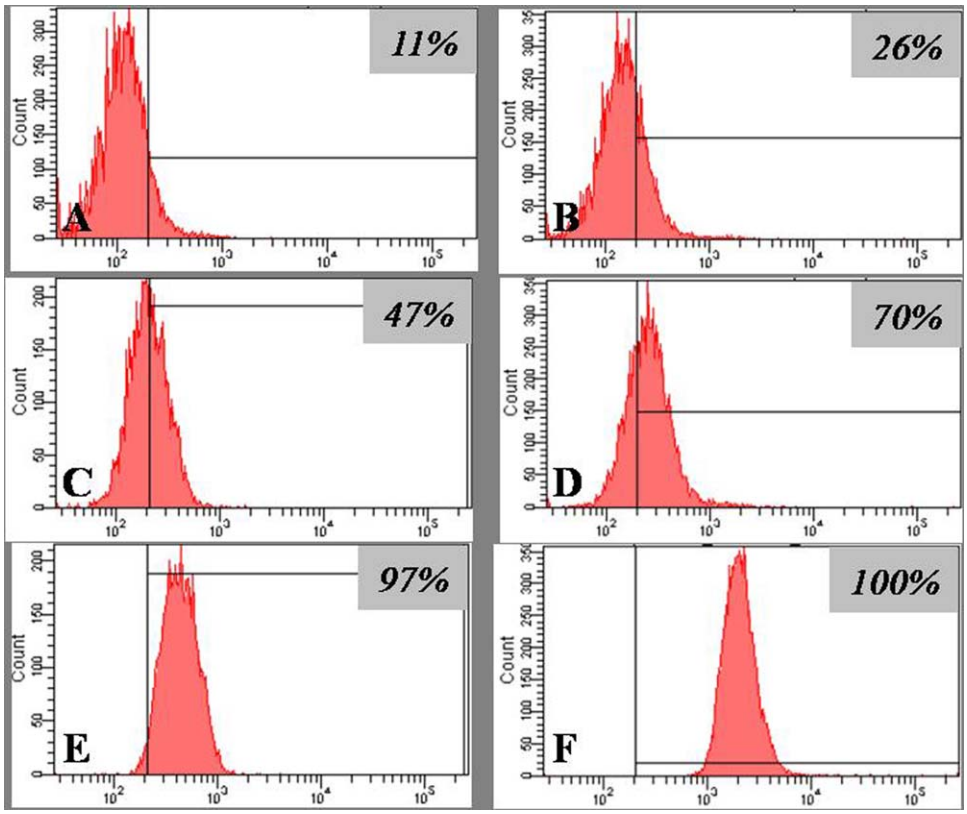

Figure 8. Flow cytometric profiles of the HepG2 cells after (A) 0, (B) 10, (C) 30, (D) 60, (E) 120, and (F) 180 min incubation with the M(Pt) micelles labeled with RhB. [Color figure can be viewed in the online issue, which is available at wileyonlinelibrary.com.]

undetectable levels 5 min after the injection of free cisplatin, whereas a considerable amount of Pt was observed even 9 h after the administration of the M(Pt) micelles.

Platinum Biodistribution in Organs and Tumor Tissues

To study the biodistribution of Pt micelles *in vivo,* we harvested the main viscera, such as the heart, liver, spleen, and kidneys, at different time points (1, 3, 6, and 24 h) after the mice were injected intravenously with a single dose of free cisplatin (Pt 5 mg/kg) and M(Pt) micelles (Pt 5 mg/kg) and determined the Pt concentrations in the samples with ICP-MS. As shown in Figure 11(A,B), a significantly greater Pt accumulation was seen in the liver and kidney tissue for the M(Pt) micelles group than in the animals treated with free cisplatin; this indicated that more micelles than free cisplatin were taken up by the reticuloendothelial system (RES) in the liver, and most metabolized platinum species were excreted through the kidneys.

Figure 11(C) shows the Pt concentration changes in the tumor tissue after the intravenous injection of cisplatin (5 mg/kg Pt) and M(Pt) micelles (5 mg/kg Pt). The Pt concentration versus time curves of the M(Pt) micelle groups were above that of the cisplatin group. Because the M(Pt) micelle did not have a

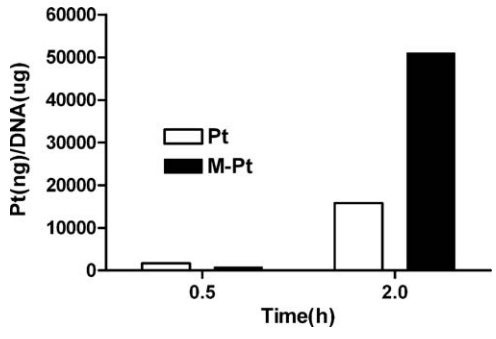

Figure 9. Pt content in the DNA collected from the HepG2 cells treated with cisplatin (Pt) and M(Pt) micelles.

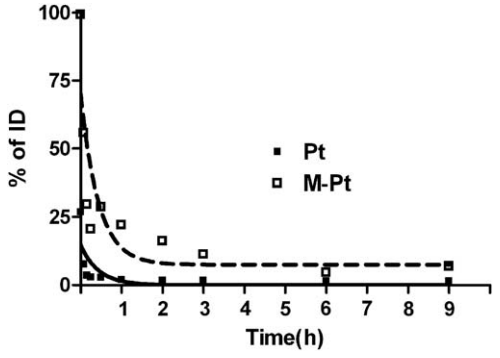

Figure 10. Blood clearance of the free cisplatin (Pt) and M(Pt) micelles. The M(Pt) micelles indicated a longer circulation time compared to that of cisplatin; this was mainly ascribed to the nanoscale size of the polymer micelles formed by mPEG-*b*-PCPGE/Pt. It is well known that the mPEG shell can increase the lift time of drugs in the blood. This prolonged circulation time benefitted the accumulation of the drug in the tumor site because of the EPR effect.

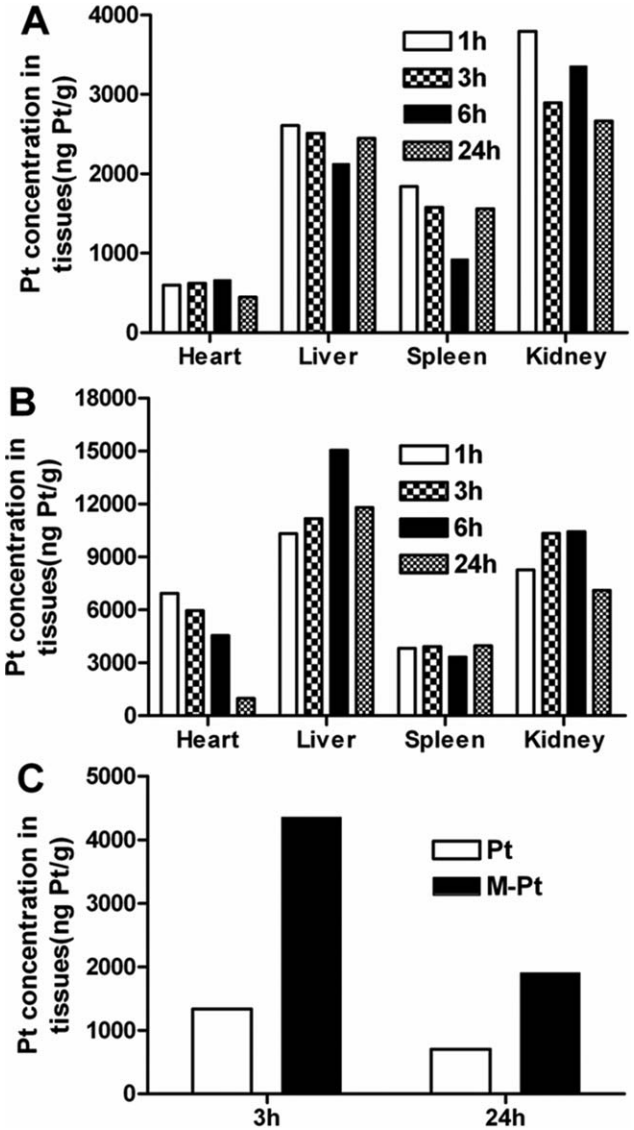

Figure 11. Biodistribution of (A) cisplatin and (B) M(Pt) micelles in the heart, liver, spleen, and kidney and the (C) Pt content with the cisplatin (Pt) and M(Pt) micelles from the H22 tumor. The content of cisplatin in the kidney was higher than that of the other organs (including the heart, liver, and spleen); that is, the main reason of renal toxicity result from cisplatin. Although the M(Pt) micelles with nanoscale size could reduce the systemic toxicity and enhance the content of Pt in tumor site.

function of active targeting, such a targeting effect was ascribable to a passive one because of the enhanced penetration and retention (EPR) effect of the tumor to the M(Pt) micelles.

In Vivo Antitumor Efficacy

To study the *in vivo* antitumor effects of the M(Pt) micelles, H22 xenograft models of the hepatocarcinoma were established by the injection of H22 cells into the lateral aspect of the anterior limb of the KM mice. When the tumor grew to a size of 50–200 mm^3 5 days after inoculation of the cancer cells, the mice were randomly divided into three groups with five mice in each group. An equivalent dose of Pt (3 mg/kg) was given three times (on days 1, 3, and 5) via intravenous injection in the tail, and the tumor sizes were measured every other day. Figure 12(A,B) shows the tumor size as a function of time. As shown in Figure 12(B), it was notable that the administration of M(Pt) micelles was relatively more efficacious than the free cisplatin in tumor suppression. This was supported by the formation of more Pt–DNA adducts (Figure 9) in the cancer cells and was consistent with the enhanced accumulation in the tumor bed [Figure 11(C)] and the longer blood circulation for micelles (Figure 10) observed previously. Figure 12(C) depicts the relative body weight changes of the mice during the test. Among all of the test

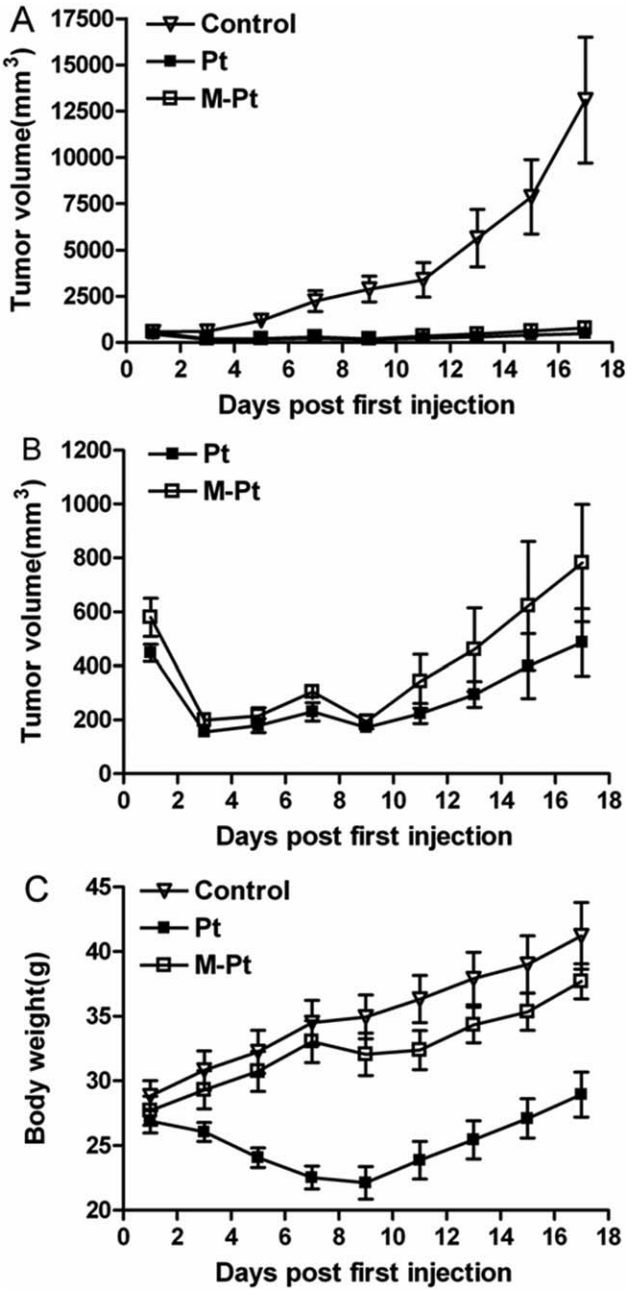

Figure 12. (A) Effect of the cisplatin (Pt, 3 mg of Pt/kg, $n = 5$), M(Pt) micelles (3 mg of Pt/kg, $n = 5$), and 0.9% saline (blank, $n = 5$) on the growth of H22 tumors inoculated in the KM mice. Each formulation was administered on days 1, 3, and 5 by intravenous injection, with the day of the first injection counted as day 1. The mean values of the data are presented. (B) Curve from the cisplatin (Pt) and M(Pt) micelles. (C) Body weight changes with time of the H22 tumor-bearing mice.

groups, the cisplatin group mice showed serious weight loss because it caused the highest systemic toxicity. In all of the other groups, the mice showed little weight loss and even gained body weight constantly because of the lower systemic toxicity.

CONCLUSIONS

In this study, polymeric micelles with cisplatin were prepared by the complexation of platinum with carboxylic groups on functionalized PEG. The drug molecules were wrapped in the core part of the micelles and protected effectively in the blood circulation. *In vivo* blood clearance showed that the micelles exhibited longer blood circulation than the free drug. Biodistribution studies showed that the polymeric micelles led to an increase in the Pt content at the tumor site, in tumor cells, and in the DNA of the tumor cells in comparison with the free cisplatin, and consequently, they displayed a substantially better antitumor efficacy. In a short, this simple complex of Pt drug with PEG made crosslinked M(Pt) micelles suitable for protecting the drugs from premature release during blood circulation and ideal for the intracellular delivery of platinum drugs.

ACKNOWLEDGMENTS

Financial support was provided by the National Natural Science Foundation of China (contract grant numbers 91227118 and 21004062).

REFERENCES

1. Cicin, I.; Saip, P.; Eralp, Y.; Selam, M.; Topuz, S.; Ozluk, Y.; Aydin, Y.; Topuz, E. *Gynecol. Oncol.* **2008**, *108*, 136.
2. Wheate, N. J.; Walker, S.; Craig, G. E.; Oun, R. *Dalton Trans.* **2010**, *39*, 8113.
3. Wang, D.; Lippard, S. *J. Nature Rev. Drug Discov.* **2005**, *4*, 307.
4. Ibrahim, A.; Hirschfeld, S.; Cohen, M. H.; Griebel, D. J.; Williams, G. A.; Pazdur, R. *Oncologist* **2004**, *9*, 8.
5. Tong, R.; Cheng, J. *J. Polym. Rev.* **2007**, *47*, 345.
6. Huynh, V. T.; Quek, J. Y.; de Souza, P. L.; Stenzel, M. H. *Biomacromolecules* **2012**, *13*, 1010.
7. Mlcouskova, J.; Kasparkova, J.; Suchankova, T.; Komeda, S.; Brabec, V. *J. Inorg. Biochem.* **2012**, *114*, 15.
8. Paczosa-Bator, B.; Cabaj, L.; Piech, R.; Skupien, K. *Analyst* **2012**, *137*, 5272.
9. Zhang, D. H.; Wang, J.; Chen, S. F.; Cheng, X. J.; Li, T. C.; Zhang, J. H.; Zhang, A. Q. *Langmuir* **2012**, *28*, 16772.
10. Liu, J. H.; Zhang, Y. W.; Lu, L. H.; Wu, G.; Chen, W. *Chem. Comm.* **2012**, *48*, 8826.
11. Yang, J.; Mao, W. W.; Sui, M. H.; Tang, J. B.; Shen, Y. Q. *J. Controlled Release* **2011**, *152*, E108.
12. Hong, W.; Kim, K.; Jung, Y.; Kim, J.; Kang, S.; Chun, J.; Chun, M.; Yim, H.; Kang, D.; Kim, T. *Eur. J. Cancer* **2012**, *48*, S172.
13. Yan, L. S.; Yang, L. X.; He, H. Y.; Hu, X. L.; Xie, Z. G.; Huang, Y. B.; Jing, X. B. *Polym. Chem.* **2012**, *3*, 1300.
14. Pati, D.; Shaikh, A. Y.; Hotha, S.; Sen Gupta, S. *Polym. Chem.* **2011**, *2*, 805.
15. Wang, X. Y.; Guo, Z. *J. Chem. Soc. Rev.* **2013**, *42*, 202.
16. Asharani, P. V.; Yi, L. W.; Gong, Z. Y.; Valiyaveettil, S. *Nanotoxicology* **2011**, *5*, 43.
17. Gehrke, H.; Pelka, J.; Hartinger, C. G.; Blank, H.; Bleimund, F.; Schneider, R.; Gerthsen, D.; Brase, S.; Crone, M.; Turk, M.; Marko, D. *Arch. Toxicol.* **2011**, *85*, 799.
18. Teow, Y.; Valiyaveettil, S. *Nanoscale* **2010**, *2*, 2607.
19. Brown, S. D.; Nativo, P.; Smith, J. A.; Stirling, D.; Edwards, P. R.; Venugopal, B.; Flint, D. J.; Plumb, J. A.; Graham, D.; Wheate, N. J. *J. Am. Chem. Soc.* **2010**, *132*, 4678.
20. Bryde, S.; de Kroon, A. *Future Med. Chem.* **2009**, *1*, 1467.
21. Pelka, J.; Gehrke, H.; Esselen, M.; Turk, M.; Crone, M.; Brase, S.; Muller, T.; Blank, H.; Send, W.; Zibat, V.; Brenner, P.; Schneider, R.; Gerthsen, D.; Marko, D. *Chem. Res. Toxicol.* **2009**, *22*, 649.
22. Hamasaki, T.; Kashiwagi, T.; Imada, T.; Nakamichi, N.; Aramaki, S.; Toh, K.; Morisawa, S.; Shimakoshi, H.; Hisaeda, Y.; Shirahata, S. *Langmuir* **2008**, *24*, 7354.
23. Wang, Y. M.; Sato, H.; Adachi, I.; Horikoshi, I. *J. Pharm. Sci.* **1996**, *85*, 1204.
24. Tomalia, D. A.; Reyna, L. A.; Svenson, S. *Biochem. Soc. Trans.* **2007**, *35*, 61.
25. Lin, X.; Zhang, Q.; Rice, J. R.; Stewart, D. R.; Nowotnik, D. P.; Howell, S. B. *Eur. J. Cancer* **2004**, *40*, 291.
26. Caldwell, G.; Neuse, E. W.; van Rensburg, C. E. J. *J. Inorg. Organomet. Polym.* **1997**, *7*, 217.
27. Cabral, H.; Nishlyama, N.; Kataoka, K. *J. Controlled Release* **2007**, *121*, 146.
28. Obermeier, B.; Frey, H. *Bioconjug. Chem.* **2011**, *22*, 436.
29. Hruby, M.; Konak, C.; Ulbrich, K. *J. Appl. Polym. Sci.* **2005**, *95*, 201.
30. Duncan, R. *Nat. Rev. Drug Discov.* **2003**, *2*, 347.
31. Cho, K. J.; Wang, X.; Nie, S. M.; Chen, Z.; Shin, D. M. *Clin. Cancer Res.* **2008**, *14*, 1310.
32. Xie, Z.; Hu, X.; Chen, X.; Lu, T.; Liu, S.; Jing, X. *J. Appl. Polym. Sci.* **2008**, *110*, 2961.
33. Xie, Z.; Lu, T.; Chen, X.; Lu, C.; Zheng, Y.; Jing, X. *J. Appl. Polym. Sci.* **2007**, *105*, 2271.
34. Xiao, H. H.; Zhou, D. F.; Liu, S.; Zheng, Y. H.; Huang, Y. B.; Jing, X. B. *Acta Biomater.* **2012**, *8*, 1859.
35. Cabral, H.; Matsumoto, Y.; Mizuno, K.; Chen, Q.; Murakami, M.; Kimura, M.; Terada, Y.; Kano, M. R.; Miyazono, K.; Uesaka, M.; Nishiyama, N.; Kataoka, K. *Nat. Nanotechnol.* **2011**, *6*, 815.
36. Xiao, H. H.; Song, H. Q.; Zhang, Y.; Qi, R. G.; Wang, R.; Xie, Z. G.; Huang, Y. B.; Li, Y. X.; Wu, Y.; Jing, X. B. *Biomaterials* **2012**, *33*, 8657.
37. Wang, R.; Hu, X. L.; Wu, S.; Xiao, H. H.; Cai, H. D.; Xie, Z. G.; Huang, Y. B.; Jing, X. B. *Mol. Pharm.* **2012**, *9*, 3200.
38. Xiao, H. H.; Song, H. Q.; Yang, Q.; Cai, H. D.; Qi, R. G.; Yan, L. S.; Liu, S.; Zheng, Y. H.; Huang, Y. B.; Liu, T. J.; Jing, X. B. *Biomaterials* **2012**, *33*, 6507.
39. Yue, J.; Li, X.; Mo, G.; Wang, R.; Huang, Y.; Jing, X. *Macromolecules* **2010**, *43*, 9645.